PLOS ONE

RESEARCH ARTICLE

Trans-synaptic degeneration in the optic pathway. A study in clinically isolated syndrome and early relapsing-remitting multiple sclerosis with or without optic neuritis

Marco Puthenparampil[1☯]*, Lisa Federle[1☯], Davide Poggiali[1], Silvia Miante[1], Alessio Signori[2], Elisabetta Pilotto[3], Francesca Rinaldi[1], Paola Perini[1], Maria Pia Sormani[2], Edoardo Midena[3], Paolo Gallo[1]

1 Multiple Sclerosis Centre, Department of Neurosciences DNS, University Hospital–Medical School, Padova, Italy, **2** Department of Health Sciences, Section of Biostatistics–University of Genova, Genova, Italy, **3** Ophthalmology Unit, Department of Neurosciences DNS, University Hospital–Medical School, Padova, Italy

☯ These authors contributed equally to this work.
* marco.puthenparampil@studenti.unipd.it

OPEN ACCESS

Citation: Puthenparampil M, Federle L, Poggiali D, Miante S, Signori A, Pilotto E, et al. (2017) Trans-synaptic degeneration in the optic pathway. A study in clinically isolated syndrome and early relapsing-remitting multiple sclerosis with or without optic neuritis. PLoS ONE 12(8): e0183957. https://doi.org/10.1371/journal.pone.0183957

Editor: Radouil Tzekov, Roskamp Institute, UNITED STATES

Received: September 5, 2016

Accepted: August 15, 2017

Published: August 29, 2017

Data Availability Statement: All relevant data are within the paper and its Supporting Information files.

Funding: This research was supported by grants from the Italian Minister of Public Health, Project GR-2010-2313255.

Competing interests: Puthenparampil Marco received travel grant from Novartis, Genzyme, Biogen Idec, Teva and Sanofi Aventis; he has been consultant for Genzyme. Federle Lisa has received

Abstract

Objective

Increasing evidence suggest that neuronal damage is an early and diffuse feature of Multiple Sclerosis (MS) pathology. Analysis of the optic pathway may help to clarify the mechanisms involved in grey matter damage in MS. Purpose of our study was to investigate the relationship between inflammation and neurodegeneration and to achieve evidence of trans-synaptic degeneration in the optic pathway in MS at clinical onset.

Methods

50 clinically isolated syndromes/early relapse-onset MS (CIS/eRRMS) with mean disease duration of 4.0±3.5 months, 28 MRI healthy controls (HC) and 31 OCT-HC were studied. Ten patients had optic neuritis at presentation (MSON+), 40 presented with other symptoms (MSON-). MRI examination included 3D-T1, 3D-FLAIR and 3D-DIR sequences. Global cortical thickness (gCTh), pericalcarin CTh (pCTh) and white matter volume (WMV) were analysed by means of Freesurfer on 3D-T1 scans. Optic radiation morphology (OR) and volume (ORV) were reconstructed on the base of the Jülich's Atlas. White matter lesion volume (WMLV), OR-WMLV and percent WM damage (WMLV/WMV = WMLV% and OR-WMLV/ORV = ORWMLV%) were obtained by 3D-FLAIR image segmentation. 3D-DIR sequences were applied to identify inflammatory lesions of the optic nerve. Optic coherence tomography (OCT) protocol included the analysis of global peripapillary retinal nerve fiber layer (g-RNFL) and the 6 *fundus oculi*'s sectors (temporal, T-RNFL; temporal superior, TS-RNFL; nasal superior, NS-RNFL; nasal, N-RNFL; nasal inferior, NI-RNFL, temporal inferior, TI-

funding for travel from Novartis, Merck Serono, Biogen Idec, Sanofi-Aventis, Bayer Schering Pharma, Almirall, Genzyme, Teva and honoraria from Genzyme, Merk Serono, Teva and Almirall. Poggiali Davide received travel grant from Biogen Idec, Novartis, Sanofi Aventis and Teva. Miante Silvia received travel grant form Biogen Idec, Novartis, Sanofi Aventis and Teva. Signori Alessio has nothing to disclose. Pilotto Elisabetta has nothing to disclose. Rinaldi Francesca serves as an advisory board member of Biogen-Idec and has received funding for travel and speaker honoraria from Merck Serono, Biogen Idec, Sanofi-Aventis, Teva and Bayer Schering Pharma. Perini Paola has received funding for travel and speaker honoraria from Merck Serono, Biogen Idec, Sanofi-Aventis, and Bayer Schering Pharma and has been consultant for Merck Serono, Biogen Idec and Teva. Sormani Maria Pia received personal fees from Merck Serono, Biogen, Novartis, Genzyme, Teva, Synthon, Roche. Midena Edoardo has nothing to disclose. Gallo Paolo has been a consultant for Bayer Schering, Biogen Idec, Genzyme, Merck Serono and Novartis; has received funding for travel and speaker honoraria from Merck-Serono, Biogen Idec, Sanofi-Aventis, Novartis Pharma and Bayer-Schering Pharma, Teva; has received research support from Bayer, Biogen Idec/Elan, Merk Serono, Genzyme and Teva; and has received research grant from the University of Padova, Veneto Region of Italy, the Italian Association for Multiple Sclerosis, the Italian Ministry of Public Health. These competing of interests do not alter our adherence to PLOS ONE policies on sharing data and materials.

RNFL). The retina of both eyes was analyzed. The eyes of ON+ were further divided into affected (aON+) or not (naON+).

Results

No difference in CTh was found between CIS/eRRMS and HC, and between MSON+ and MSON-. Moreover, MSON+ and MSON- did not differ for any WM lesion load parameter. The most significant correlations between RNFL thickness and optic radiation WM pathology were found in MSON+. In these patients, the temporal RNFL inversely correlated to ipsilateral optic radiation WM lesion load (T-RNFL: r -0.7, $p<0.05$; TS-RNFL: r -0.7, $p<0.05$), while nasal RNFL inversely correlated to contralateral optic radiation WM lesion load (NI: r -0.8, $p<0.01$; NS-RNFL: r -0.8, $p<0.01$).

Conclusions

Our findings suggest that in MSON+ the optic pathway is site of a diffuse pathological process that involves both directly and via trans-synaptic degeneration the RNFL.

Introduction

Increasing evidence suggests that grey matter (GM) is early and widely damaged in Multiple Sclerosis (MS). Histological and neuroimaging studies have disclosed variable degrees of inflammation [1–3] and diffuse neurodegeneration (atrophy) [4,5] in the cortex of MS patients, even at clinical onset and sometimes preceding the appearance of white matter (WM) lesions [6]. Cortical inflammation may be the cause of neuronal loss and GM atrophy. Nevertheless, retrograde or anterograde axonal degeneration, starting within WM lesions far from the cortex or in the normal appearing WM (NAWM), may also be responsible for neuronal loss and GM atrophy [7].

Due to its anatomical complexity, characterized by both WM and GM inter-connected structures, the optic pathway may offer the possibility of investigating the complex relationship between axonal damage in WM lesions and neuronal loss [8]. However, studies aimed at disclosing correlations between optical coherence tomography (OCT) and magnetic resonance imaging (MRI) findings have reported conflicting results. Indeed, the association between WM lesion volume (WMLV) in the optic radiation and retinal or cortical damage (suggested to be the expression of trans-synaptic degeneration) that was observed in several studies [7,9–13], was not be confirmed by Raz et al [14]. Several factors related to the methodology used, the patient populations analyzed (different disease duration and age) and the variable degrees of WM and GM lesion load in the optic pathway may explain literature discrepancies.

The predictive clinical values of any inflammatory or neurodegenerative parameter, as well as the possible relationship between WM and GM pathology, should be analyzed in the very early MS phases, possibly at clinical onset. Indeed, with MS progression the demonstration of any possible correlation between axonal damage in the WM, trans-synaptic degeneration and cortical atrophy is hampered by the widespread diffusion of both WM and GM pathology. Therefore, we analyzed the possible relationships between WM and GM pathology in the optic pathway in 50 patients with clinically isolated syndrome (CIS) or very early relapse-onset MS (eRRMS) in order to set the basis for a longitudinal study.

Material and methods

Study population

Fifty consecutive patients with a diagnosis of CIS suggestive of MS or eRRMS according to the most recent criteria [15] were included in the study. Diagnostic work-up included MRI (see below), Visual Evoked Potentials (VEP), detailed biochemical, immunological (including anti-extractable nuclear antibodies, anti-nuclear antibodies, Anti-neutrophil cytoplasmic antibodies, Angiotensin Converting Enzyme, anti-Phospholipid antibodies, anti-Aquaporin4 antibodies, Ab, anti-native DNA antibodies, anti-thyroid peroxidase antibodies, anti-thyroglobulin antibodies, anti-TSH Receptor antibodies, IgA-IgE-IgM-IgG concentration, C3, C4, circulating immunocomplex) and microbiological screenings in blood, and cerebrospinal fluid examination (i.e. albumin, IgG and glucose concentrations, cell count, IgG Index and IgG Hyperbolic Function, IsoElettroFocusing for detection of IgG Oligoclonal Bands (IgGOB); microbiological tests when necessary). Inclusion criteria were also disease duration < 12 months and age ≥ 18 years. Exclusion criteria included any systemic (including diabetes), ophthalmological (severe myopia: $>$ -6.0 dp or axial eye length $>$26mm; severe hypermetropia: $>$ 5 dp; cylinder $>$3 dp; optic disc drusen; cataracts; current or previous glaucoma; other causes of vision loss not attributable to MS) and drug-related causes of retinal damage. Patient's OCT and MRI findings were compared to those of two independent cohort of 31 and 28 healthy controls (HC) respectively (hereafter abbreviated in HC-OCT and HC-MRI). Patients and HC did not differ for age and gender. The study was approved by the Ethics Committee of Azienda Ospedaliera di Padova and a written informed consent was obtained by all the participants.

MRI protocol

Images were acquired using a 3Tesla MRI (Ingenia, Philips Medical Systems, Best, The Netherlands) with 33 mT/m power gradient and a 32-channel head coil. No major hardware upgrades occurred during the study, and bimonthly quality-assurance sessions assured measurement stability. The following images were acquired: (a) three-dimensional (3D) Fluid Attenuated Inversion Recovery (FLAIR): Repetition Time (RT) 4800 ms; Echo Time (ET) 310 ms; Inversion Time (IT) 1650 ms; 365 contiguous sagittal slices with thickness of 1.0 mm; matrix size 512 x 512; and FOV = 256 x 256 x 365 mm^3; (b) 3D-turbo field echo T1 (TFE, 3D-T1): RT 7.8 ms; ET 3.6 ms; 180 contiguous sagittal slices with the off-centre positioned on zero with thickness of 1.0 mm; flip angle = 8°; matrix size = 220 x 220; and FOV = 220 x 220 x 180 mm^3; (c) 3D-Double Inversion Recovery (DIR) sequences: RT 5500 ms; ET 280 ms; 300 contiguous sagittal slices with the off-centre positioned on zero with thickness of 1.3 mm; flip angle = 90°; matrix size = 256 x 256; and FOV = 256 x 256 x 390 mm^3; d) T2-weighted with combined fat and water suppression SPIR/FLAIR (8000/120 [TR/TE]; TI, 2200; field of view, 160mm2; matrix, 2562; signal average, 2; echo train length, 21; imaging time, 4 minutes) for the identification of high-signal lesions within the optic nerve. However, on the base of the results of two recent studies [16,17] that disclosed the superiority of 3D DIR sequence in detecting optic nerve lesions compared to FLAIR images, we used both sequences to depict optic nerve lesions. This was done by two independent observers (MP and DP) blinded to patient clinical data. All patients and HC were analysed twice to evaluate the intra-observer variability.

Both global cortical thickness (gCTh) and pericalcarin CTh (pCTh) were analysed by means of Freesurfer on 3D-T1 sequences. The WM volume (WMV) was also calculated by Freesurfer on 3D-T1 sequences, while the application of the Jülich probabilistic atlas (threshold at 0.2) to the same sequences allowed obtaining a binary masks of the optic radiations in

the standard Montreal Neurological Institute space. This mask was then projected into the space of individual subjects to obtain the optic radiation volume (ORV). White matter lesions were identified in the space of individual subjects by consensus of three examiners (MP, DP, PG) and their volumes were calculated by a Python script. Optic radiation WMLV were obtained by the intersection of WM lesion mask and optic radiation mask. Furthermore, the WMLV/WMV ratio (WMLV%) and the optic radiation WMLV/ORV ratio (optic radiation WMLV%) were also calculated. Finally, in order to avoid the influence of global WMLV on optic radiation WMLV, the ratio between optic radiation WMLV% and global WMLV% was calculated (WMLV-ratio).

OCT protocol

Spectral Domain retinal OCT (SPECTRALIS; Heidelberg Engineering, Carlsbad, CA; Heidelberg Eye Explorer version 1.7.0.0) examination of each eye was performed in all patients and controls by two observers (FL and PE). All the OCT scans fulfilled OSCAR-IB criteria [18,19]. OCT scans were acquired in a dark room, without the administration of any mydriatic agent. OCT scans included a peri-papillary 3.5 mm ring scan to measure retinal nerve fiber layer (RNFL) thickness, which was expressed both as global peri-papillary RNFL (g-RNFL) and as sectorial peri-papillary RNFL (temporal, T-RNFL; temporal superior, TS-RNFL; nasal superior, NS-RNFL; nasal, N-RNFL; nasal inferior, NI-RNFL); temporal inferior, TI-RNFL). The ring scan was manually superimposed to the optic nerve head. To exclude the presence of artifacts that interfered with RNFL segmentation and in order to confirm the automatic RNFL segmentation, an expert (FL or EP) reviewed all the OCT scans.

We analyzed the possible correlations between the temporal (T, TI, TS) and the nasal (N, NI, NS) fields of the RNFL respectively with the ipsilateral and the contralateral optic radiation WM pathology (WMLV and WMLV%), and between all RNFL sectors with global WMLV and WMLV%.

Statistical analysis

Mean and standard deviation (SD) or median and interquartile range (IQR) were reported for continuous variables. Correlation between temporal, nasal and MRI values was calculated by mean of Pearson's coefficient. To assess differences between groups for the clinical variables investigated and to highlight association between both temporal and nasal parameters and MRI characteristics (WMLV, WMLV%, ORWMLV, ORWMLV%, WMLV-ratio) a Generalized estimating equation (GEE) model was performed. Choice of GEE model was adopted to take in account the correlation between observations originated from the same patient (left and right eye). To statistically test whether correlation between temporal (or nasal) values and resonance magnetic parameters (MRI variables, namely WMLV (mm3), WMLV%, OR-WMLV (mm3), OR-WMLV%, OR-WMLV% / WMLV%, pericalcarinCTh and global Cth) was significantly different across the subgroups (MSON+ and MSON-), an interaction term between subgroups and MRI parameters was introduced into the GEE model. The unstructured correlation matrix was used as correlation structure for GEE model. The RNFL parameters were used as dependent variable in the GEE model.

Analysis of variance (ANOVA) was used to compare global CTh between groups (no different values within same patient). Since MRI values showed a strongly skewed distribution, a cube root transformation was adopted before the correlation analysis and GEE models. A p-value lower than 0.05 was considered statistically significant. Stata (v.13; StataCorp) has been used for the computation.

Table 1. Clinical and demographic parameters of all the subjects included in the study.

	Patients			Controls	
	CIS/eRRMS	***MSON+***	***MSON-***	***HC-OCT***	***HC-MRI***
number	50	10	40	31	28
age (years) mean ± dev.st (range)	34.2±10.5 (18–59)	34.3±10.7 (22–56)	34.2±10.6 (18–59)	35.4±9.1 (25–59)	36.1±14.1 (18–66)
female/male ratio	1.8	1.5	1.9	1.4	3.7
CIS suggestive of MS/eRRMS	29/21	5/5	24/16	n.a	n.a.
disease duration (months) mean ± dev.st	4.0 ± 3.5	4.5 ±4.1	3.9 ± 3.3	n.a.	n.a.
EDSS median	1.5 (1–4)	1.25 (1–2.5)	2 (1–4)	n.a.	n.a.
IgGOB (%)	32 (64%)	6 (60%)	26 (65%)	0 (0%)	0 (0%)
delay onset-MRI (months) mean ± dev.st	4.0 ± 3.5	4.5 ±4.1	3.9 ± 3.3	n.a.	n.a.
delay onset-OCT (months) mean ± dev.st	4.6 ± 3.5	5.8 ± 4.0	4.2 ± 3.3	n.a.	n.a.
delay MRI-OCT (months) mean ± dev.st	0.64 ± 1.10	1.00 ± 0.94	0.55 ± 1.13	n.a.	n.a.

No significant difference was observed in any of the listed parameters between patient's groups and controls, except for a mild difference between MRI-OCT delay between MSON- and MSON+. Abbreviations: Clinically Isolated Syndrome: CIS; early-Relapsing Remitting Multiple Sclerosis: eRRMS; Optic Neuritis patients: MSON+; Not Optic Neuritis patients: MSON-; MRI-Healty Control: HC-MRI; OCT-Healthy Control: HC-OCT; Expanded Disability Status Scale: EDSS; IgG Oligoclonal Bands: IgGOB; not applicable: n.a..

https://doi.org/10.1371/journal.pone.0183957.t001

Results

Study population

No difference in the demographic features was observed among the groups of patients (Table 1, S1 Table). All patients presented a negative immunological and microbiological screening, while IgGOB were detected in 32 (64%) patients. Based on the clinical presentation, the patients were divided in two groups: 1) 'optic neuritis' MS onset (MSON+), this group was composed by 10 patients who had an acute or subacute monocular visual loss associated with retro-orbital pain during eye movement with an ophthalmological evaluation and a static perimetry confirming the diagnosis [20]; 2) 'not optic neuritis' MS onset (MSON-), 40 patients.

Interestingly, a clear-cut separation of the two groups was also achieved on the base of the MRI image of the optic nerve. Indeed, an inflammatory lesion in the affected optic nerve was observed on DIR images in all MSON+ patients by two independent evaluators blinded to clinical history, while no signal abnormality was found in the optic nerves of MSON- patients. The contribution of 3D-DIR in optic nerve lesion detection was confirmed to be particularly significant, with 100% accuracy for both operators and 0% intra-observer and inter-observer variability (Fig 1).

White matter and cortical findings

WM lesions in the optic radiations were detected in 36/40 (90.0%) MSON- patients and 9/10 (90.0%) MSON+ patients (p = 0.99). No difference in WM pathology (i.e., global WMLV, optic radiation WMLV, global WMLV%, optic radiation WMLV%) was observed between the groups (Table 2).

Moreover, no difference between MSON+, MSON- and HC-MRI in both global and pericalcarin CTh was observed (p = 0.31 and p = 0.18 respectively, Table 3). Finally, no correlation was demonstrated between global or pericalcarin CTh and all metrics of WM pathology, age and gender.

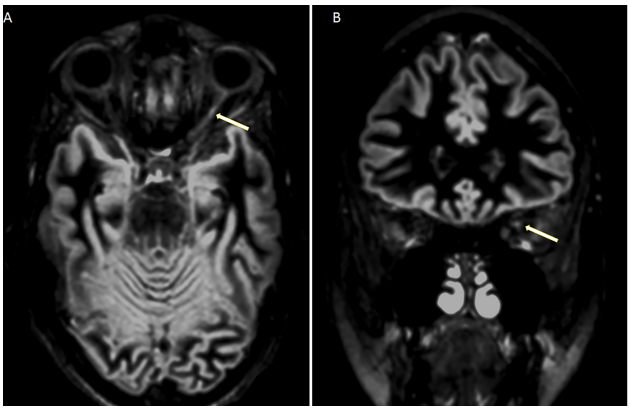

Fig 1. Double inversion recovery images (A Axial and B coronal) showing an inflammatory lesion (hyperintense signal) in the left optic nerve (arrows).

https://doi.org/10.1371/journal.pone.0183957.g001

RNFL

No difference in any OCT parameter was found between female and male subjects in each study group (HC-OCT, MSON+, MSON-) as well as no correlation between RNFL thickness and age was observed in patients and controls.

A thinner g-RNFL was observed in the affected eyes of MSON+ (83.3±25.3 μm) compared to both HC-OCT (99.6±9.3 μm, $p<0.001$) and MSON- (99.8±9.1 μm, $p<0.001$). Moreover, the affected eyes of MSON+ presented a significant thinning of T-RNFL, TI-RNFL and TS-RNFL (Fig 2, S2 Table) compared to their not affected eyes and to the eyes of HC-OCT and MSON-. Finally, the not affected eyes of both MSON+ and MSON- did not differ in RNFL thinning compared to the eyes of HC-OCT.

Correlation between RNFL thickness and WM parameters

All the correlation data between RNFL findings and WM pathology parameters are reported in Table 4 (all raw data are enclosed as S3 Table). The most significant correlations were found between the temporal (TI and T-RNFL) sectors and both global and optic radiation WMLV and WMLV%. With regard to the nasal sectors, NI and NS mildly correlated with contralateral optic radiation WMLV and WMLV%.

Table 2. White matter MRI parameters in MSON+ and MSON-. Results are reported as median (IQR). P-values were obtained from GEE model. GEE analysis was performed at eye-level. White Matter Lesion Volume: WMLV; percentage of WMLV: WMLV%; optic radiation WMLV: OR-WMLV; percentage of OR-WMLV: OR-WMLV%. Other abbreviations as in Table 1.

	MSON+	*MSON-*	*p*
WMLV (mm^3)	1369.3 (698.5–2816.2)	1721.4 (599.4–10716.7)	0.31
WMLV%	0.3 (0.1–0.6)	0.3 (0.1–2.3)	0.34
OR-WMLV (mm^3)	74.3 (8.8–229.5)	72.3 (8.7–573.1)	0.24
OR-WMLV%	0.3 (0.03–0.9)	0.3 (0.03–2.0)	0.25
OR-WMLV% / WMLV%	0.87 (0.18–1.66)	0.88 (0.15–2.47)	0.97

https://doi.org/10.1371/journal.pone.0183957.t002

Table 3. Cortical thickness values in MSON-, HC-MRI and MSON+.

Corticalareas		MSON- (mm)	HC-MRI (mm)	MSON+ (mm)	p-value
Pericalcarin CTh	(mean ± st.dev.)	1.70 ± 0.18	1.76 ± 0.20	1.66 (0.17)	0.28
Global CTh	(mean ± st.dev.)	2.48 ± 0.12	2.47 ± 0.11	2.40 ± 0.13	0.18

No difference was found among these three groups. Cortical thickness: CTh. Other abbreviations as in Table 1.

https://doi.org/10.1371/journal.pone.0183957.t003

Stratified analysis by history of optic neuritis

The interaction analysis disclosed that lower values of TI, T and TS-RNFL associated with higher values of optic radiation WMLV ($p<0.01$, $p<0.05$ and $p<0.05$, respectively) and WMLV% ($p < 0.005$; $p < 0.05$ and $p< 0.005$, respectively) in the affected eye of MSON+ compared to MSON- eyes. Similarly, lower values of TS-RNFL ($p<0.05$) were associated to higher values of global WMLV in MSON+ affected eyes compared with MSON-.

In MSON- the correlation between RNFL and WM parameters was not confirmed. In MSON+ the temporal RNFL inversely correlated to ipsilateral optic radiation WM lesion load (T-RNFL: r -0.7, $p<0.05$; TS-RNFL: r -0.7, $p<0.05$), while nasal RNFL inversely correlated to contralateral optic radiation WM lesion load (NI: r -0.8, $p<0.01$; NS-RNFL: r -0.8, $p<0.01$).

Correlation between RNFL thickness and cortical thickness

No correlation between RNFL and CTh was observed in both affected and not affected eyes of MSON+, while in MSON- mild correlations were disclosed between gCTh and T-RNFL (r:-0.28, $p<0.05$), TS-RNFL (R:-0.35, $p<0.005$) and N-RNFL (r:0.23, $p<0.05$).

When applying the GEE analysis, the correlation between gCTh and TI-RNFL differed within groups and reached the statistical significance ($p<0.05$). The correlation was positive in the affected eye of MSON+ (r:0.55, $p = 0.10$), but was negative in MSON- (r: -0.15, $p = 0.2$). The correlation between gCTh and T-RNFL differed among the three groups with a trend toward the significance, that was not reached ($p = 0.064$).

When considering pCTh, the correlation with T-RNFL (Table 5) was positive when considering the affected eye of MSON+ (r: 0.43, $p = 0.2$) but negative in the other subgroups (i.e., r:-0.19, $p = 0.1$ in MSON- and r:-0.44, $p = 0.20$ in the MSON+ not affected eye). When applying GEE analysis, the difference among subgroups reached the significance ($p<0.05$). Finally, a trend in the correlation between TS-RNFL and pCTh ($p = 0.054$) was observed.

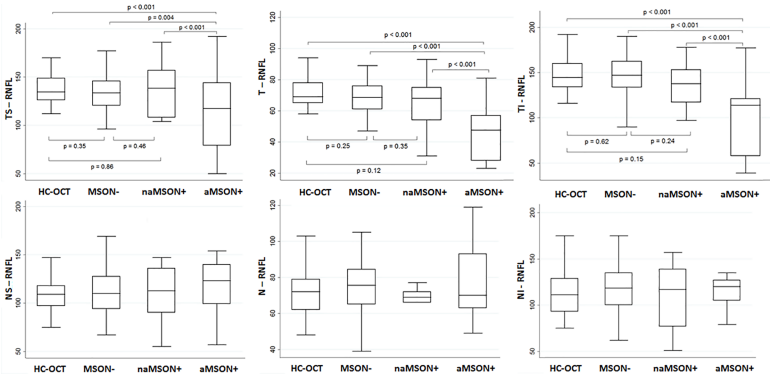

Fig 2. Comparison of the RNFL's sector values. Healthy Controls: HC-OCT; Not Optic Neuritis MS patients: MSON-; Optic Neuritis MS patients: MSON+; affected eye MSON+: aON+; not affected eye MS ON +: naON+.

https://doi.org/10.1371/journal.pone.0183957.g002

Table 4. OCT and white matter pathology correlations.

	All observation (n = 100)					
	TI-RNFL	**T-RNFL**	**TS-RNFL**	**NI-RNFL**	**N-RNFL**	**NS-RNFL**
WMLV (mm^3)	**-0.33 (0.001)**	**-0.25 (0.013)**	-0.19 (0.061)	**-0.21 (0.033)**	-0.07 (0.49)	-0.09 (0.36)
WMLV%	**-0.33 (0.001)**	**-0.24 (0.014)**	-0.19 (0.061)	**-0.23 (0.022)**	-0.09 (0.39)	-0.11 (0.29)
ORWMLV (mm3)	**-0.28 (0.006)**	**-0.20 (0.047)**	**-0.28 (0.005)**	**-0.23 (0.02)**	-0.14 (0.16)	**-0.25 (0.013)**
ORWMLV%	**-0.27 (0.006)**	-0.19 (0.055)	**-0.27 (0.007)**	**-0.24 (0.016)**	-0.15 (0.15)	**-0.24 (0.016)**
Ratio	-0.13 (0.20)	-0.05 (0.65)	**-0.25 (0.014)**	-0.19 (0.062)	-0.086 (0.40)	**-0.26 (0.001)**
	MSON–(n = 80)					
WMLV (mm^3)	-0.16 (0.15)	-0.18 (0.11)	0 (0.99)	-0.15 (0.18)	-0.12 (0.27)	0.037 (0.75)
WMLV%	-0.15 (0.20)	-0.17 (0.14)	0.01 (0.97)	-0.18 (0.10)	-0.14 (0.20)	0.02 (0.87)
ORWMLV (mm^3)	-0.14 (0.24)	-0.066 (0.56)	-0.16 (0.17)	-0.19 (0.084)	-0.12 (0.29)	-0.18 (0.11)
ORWMLV%	-0.13 (0.26)	-0.065 (0.57)	-0.15 (0.18)	-0.21 (0.066)	-0.13 (0.25)	-0.17 (0.12)
Ratio	-0.09 (0.43)	-0.004 (0.97)	-0.16 (0.17)	-0.14 (0.21)	-0.045 (0.69)	-0.20 (0.078)
	MSON + not affected eyes (n = 10)					
WMLV (mm^3)	-0.15 (0.68)	0.01 (0.97)	-0.07 (0.85)	-0.16 (0.65)	0.08 (0.83)	-0.40 (0.26)
WMLV%	-0.15 (0.68)	0.01 (0.97)	-0.07 (0.85)	-0.16 (0.65)	0.08 (0.83)	-0.40 (0.26)
ORWMLV (mm^3)	-0.52 (0.13)	-0.27 (0.46)	-0.43 (0.21)	-0.35 (0.33)	-0.07 (0.85)	-0.44 (0.20)
ORWMLV%	-0.58 (0.08)	-0.36 (0.30)	-0.50 (0.14)	-0.32 (0.36)	-0.04 (0.91)	-0.48 (0.16)
Ratio	-0.61 (0.059)	-0.46 (0.18)	**-0.73 (0.016)**	-0.31 (0.38)	-0.027 (0.94)	-0.53 (0.12)
	MSON + affected eyes (n = 10)					
WMLV (mm^3)	-0.39 (0.26)	-0.55 (0.10)	-0.54 (0.11)	**-0.70 (0.025)**	-0.17 (0.64)	-0.50 (0.14)
WMLV%	-0.39 (0.26)	-0.55 (0.10)	-0.54 (0.11)	**-0.70 (0.025)**	-0.17 (0.64)	-0.50 (0.14)
ORWMLV (mm3)	-0.44 (0.20)	**-0.66 (0.037)**	**-0.67 (0.035)**	**-0.79 (0.006)**	-0.46 (0.18)	**-0.77 (0.009)**
ORWMLV%	-0.46 (0.19)	**-0.69 (0.029)**	**-0.64 (0.044)**	**-0.76 (0.011)**	-0.44 (0.20)	**-0.75 (0.013)**
Ratio	-0.38 (0.27)	-0.63 (0.053)	**-0.64 (0.044)**	-0.49 (0.15)	-0.48 (0.16)	**-0.66 (0.038)**

The temporal RNFL sectors were correlated with the ipsilateral OR, while the nasal sectors were correlated with the contralateral OR. P-values reported for "All observations" and MSON- groups derived from GEE, which was applied in order to consider inter-eye correlation. Since within MSON+ affected and not affected eyes all observations were from independent patients, Pearson correlation was performed.

Retinal nerve fibre layer: RNFL; global RNFL: g-RNFL; temporal inferior RNFL: TI-RNFL; temporal RNFL: T-RNFL; temporal superior RNFL, TS-RNFL; nasal superior RNFL: NS-RNFL; nasal RNFL: N-RNFL; nasal inferior RNFL: NI-RNFL Other abbreviations as in Tables 1 and 2.

https://doi.org/10.1371/journal.pone.0183957.t004

Discussion

Several pathological processes may contribute to determine neurodegeneration in MS, such as GM inflammation, retrograde axonal degeneration and trans-synaptic degeneration. Indeed, variable degrees of meningeal and cortical inflammation have been described in all the clinical types of MS [21,22] and locally produced neurotoxins and pro-apoptotic signals have been proposed to play a major role in determining neuronal loss [23–26]. Axonal damage in WM lesions and in NAWM far from the cortex may also play a relevant role in neurodegeneration: an extensive axonal transection has been demonstrated in active WM lesions [27], black holes (areas of severe axonal loss) are commonly observed in T1 weighted MRI scans [28] and anterograde and/or retrograde trans-synaptic degenerations have also been suggested to contribute to neuronal loss and GM atrophy [29–32]. However, the demonstration of any possible correlation between WM damage, trans-synaptic degeneration and cortical atrophy in MS is hampered by the progressive and widespread diffusion of both WM and GM pathology with disease progression. Thus, we studied CIS highly suggestive of MS and eRRMS, with very short disease duration, not treated with disease modifying therapies and having no co-morbidity,

Table 5. Correlations between RNFL and cortical thickness.

	All observation (n = 100)					
	TI-RNFL	**T-RNFL**	**TS-RNFL**	**NI-RNFL**	**N-RNFL**	**NS-RNFL**
pCTh	0.12 (0.25)	-0.09 (0.36)	-0.06 (0.52)	0.13 (0.20)	0.08 (0.45)	0 (0.99)
gCTh	0.13 (0.21)	-0.03 (0.79)	-0.14 (0.18)	0.05 (0.61)	**0.23 (0.024)**	0.0 (0.50)
	MSON- (n = 80)					
pCTh	0.01 (0.90)	-0.19 (0.084)	-0.16 (0.17)	0.11 (0.32)	0.09 (0.42)	0.04 (0.70)
gCTh	-0.15 (0.17)	**-0.28 (0.011)**	**-0.35 (0.002)**	0.06 (0.62)	**0.26 (0.019)**	0.05 (0.69)
	MSON+ not affected eyes (n = 10)					
pCTh	0.03 (0.93)	-0.44 (0.20)	-0.47 (0.17)	0.31 (0.39)	0.25 (0.48)	0.19 (0.60)
gCTh	0.02 (0.95)	0.13 (0.72)	0.01 (0.99)	0.16 (0.67)	0.14 (0.70)	0.24 (0.51)
	MSON+ affected eyes (n = 10)					
pCTh	0.45 (0.19)	0.43 (0.21)	0.42 (0.23)	0.02 (0.96)	-0.21 (0.57)	-0.45 (0.19)
gCTh	0.55 (0.10)	0.27 (0.45)	0.19 (0.60)	-0.19 (0.60)	-0.01 (0.99)	0.19 (0.60)

The analysis was performed correlating the temporal RNFL sectors with the ipsilateral pericalcarin CTh (pCTh) and the nasal RNFL sectors with the contralateral pCTh. P-values reported for "All observations" and MSON- groups derived from GEE, which was applied in order to consider inter-eye correlation. Since within MSON+ affected and not affected eyes all observations were from independent patients, Pearson correlation was performed. All the sectors were correlated to global CTh (gCTh). Other abbreviations as in Tables 1, 2 and 4.

https://doi.org/10.1371/journal.pone.0183957.t005

and found that in MSON+ the optic pathway is likely site of a diffuse pathological process involving the RNFL either directly or via trans-synaptic degeneration.

We observed a lack of correlation between WM (global or optic radiation WM lesion load) and GM (global or pericalcarin CTh) damage. This finding questions a role for anterograde trans-synaptic degeneration in determining cortical atrophy in very early clinical MS phases. However, anterograde trans-synaptic degeneration may become more evident in later disease phases, as suggested by observations in patients with longer disease duration (i.e., 9.0 years), where a correlation between optic radiation WM lesion load and cortical volume could be observed [7].

In our study the role played by axonal damage in the NAWM, a matter of controversial debate [33], was not investigated. Recently, cortical atrophy was demonstrated to associate with a loss of NAWM integrity in MS patients with long-standing disease [34]. However, combined histopathology and MRI studies have suggested that while both demyelination and axonal damage are present in lesions, the NAWM damage particularly consists of subtle demyelination [35]. Moreover, NAWM damage was observed to increase with disease progression. Thus, we believe that, given the very short mean disease duration (4.0±3.5 months) of our cohort of CIS/eRRMS, the eventual role played by axonal damage in NAWM should be considered negligible.

The most interesting finding of our study was the observation of an inverse association between RNFL thickness and WM lesion load in the optic radiation (ipsilateral for temporal RNFL and contralateral for nasal RNFL) only in MSON+ patients. This finding seems to indicate that initial mechanism(s) of retrograde degeneration, which proceeds from retrochiasmatic structures to RNFL, may occurs in these patients. It might be possible that the combination of optic neuritis and WM damage in the optic pathway triggers trans-synaptic degenerations. The involvement of the Lateral Geniculate Nucleus (LGN) in this process is suggested by the observation of a significant neural loss in this nucleus [29], especially in the parvocellular neuron layers [36]. However, these findings could only partially be explained by retrograde degeneration, since a damage of the optic radiation accounts for a minor percentage (14–28%) of LGN volume loss [29]. Moreover, the loss of parvocellular neurons in LGN was found to

correlate with ON damage [36], thus indicating an anterograde trans-synaptic degeneration involving this nucleus and then spreading to the optic radiation, as demonstrated by connectivity changes in the optic radiation of MS patients with a previous history of optic neuritis [37].

No clear evidence of trans-synaptic (retrograde or anterograde) degeneration could be found in MSON-. Indeed, in these patients RNFL thickness did not correlate with optic radiation WMLV or pericalclarin CTh and pericalcarin CTh did not associate to optic radiation WMLV. Since the correlation between T-RNFL and gCTh did not reach the significance in all MS subgroups, the difference in affected and not-affected eye MSON+ and MSON- disclosed by GEE has be taken with caution and eventually confirmed in a larger cohort of patients. Since MSON- and MSON+ did not differ in optic radiation or global WMLV, the role played by optic neuritis seems to be pivotal within the complex pathological process occurring in the optic pathway of ON+ MS patients.

We are aware of the limitations of our study. First, the low number of MSON+ patients, that, however, is in line with the percentage of optic neuritis observed at MS onset (20–25%). Despite this limitation, the associations between RNFL thickness and WM lesion load in the optic radiation in these patients reached the statistical significance. A study on a larger cohort of MSON+ is currently in progress. Second, the lack of other OCT parameters. We point out that our study was designed to evaluate the RNFL as a possible site of neurodegeneration. Further information might rise from the analysis of macular volume and ganglion cell layer thickness, that were not included in the present study. Third, multi-focal electroretinogram and/or multi-focal visual evoked potential may help to understand the functional damage associated to neurodegeneration.

In summary, in ON+ patients the optic nerve inflammation co-operate with optic radiation WM lesion load in determining a more diffuse damage in the optic pathway, that leads to RNFL thinning and LGN neuronal loss. Trans-synaptic degeneration may be one of the mechanisms that links inflammation and neurodegeneration at least in these patients.

Supporting information

S1 Table. Clinical and demographical features of CIS/eRRMS patients.
(PDF)

S2 Table. Global and sectorial RNFL values in the 4 groups of patients. Only temporal field RNFL (TI-RNFL, T-RNFL and TS-RNFL) was reduced in affected eye of MSON+ when compared to HC, MSON- and not affected eye of ON+. No difference were found for the nasal field (NI-RNFL, N-RNFL, NS-RNFL). OCT healthy controls: HC-OCT; MS patients without previous medical history of optic neuritis: MSON-; MS patients with medical history of optic neuritis: MSON+; retinal nerve fibre layer: RNFL; global RNFL: g-RNFL; temporal inferior RNFL: TI-RNFL; temporal RNFL: T-RNFL; temporal superior RNFL, TS-RNFL; nasal superior RNFL: NS-RNFL; nasal RNFL: N-RNFL; nasal inferior RNFL: NI-RNFL. *: $p < 0.005$ when compared to affected MSON+; **: $p < 0.001$ when compared to affected MSON+.
(PDF)

S3 Table. OCT and MRI parameters of the study population.
(PDF)

Acknowledgments

The authors would like to thank the patients and staff at the Multiple Sclerosis Centre of Padua.

Author Contributions

Conceptualization: Marco Puthenparampil, Lisa Federle, Davide Poggiali, Silvia Miante, Elisabetta Pilotto, Francesca Rinaldi, Paola Perini, Maria Pia Sormani, Edoardo Midena, Paolo Gallo.

Data curation: Marco Puthenparampil, Lisa Federle, Davide Poggiali, Silvia Miante, Alessio Signori, Elisabetta Pilotto.

Formal analysis: Marco Puthenparampil, Lisa Federle, Elisabetta Pilotto, Francesca Rinaldi.

Funding acquisition: Paolo Gallo.

Investigation: Marco Puthenparampil, Lisa Federle.

Methodology: Marco Puthenparampil, Alessio Signori, Elisabetta Pilotto, Maria Pia Sormani, Edoardo Midena.

Resources: Paolo Gallo.

Software: Davide Poggiali, Alessio Signori, Maria Pia Sormani.

Supervision: Paola Perini.

Validation: Alessio Signori.

Writing – original draft: Marco Puthenparampil, Lisa Federle, Davide Poggiali, Silvia Miante, Alessio Signori, Elisabetta Pilotto, Francesca Rinaldi, Paola Perini, Maria Pia Sormani, Edoardo Midena, Paolo Gallo.

Writing – review & editing: Marco Puthenparampil, Lisa Federle, Davide Poggiali, Silvia Miante, Alessio Signori, Elisabetta Pilotto, Francesca Rinaldi, Paola Perini, Maria Pia Sormani, Edoardo Midena, Paolo Gallo.

References

1. Lucchinetti C, Brück W, Parisi J, Scheithauer B, Rodriguez M, Lassmann H. Heterogeneity of multiple sclerosis lesions: implications for the pathogenesis of demyelination. Ann Neurol [Internet]. 2000 Jun [cited 2017 Aug 22]; 47(6):707–17. Available from: http://www.ncbi.nlm.nih.gov/pubmed/10852536 PMID: 10852536
2. Calabrese M, Magliozzi R, Ciccarelli O, Geurts JJG, Reynolds R, Martin R. Exploring the origins of grey matter damage in multiple sclerosis. Nat Rev Neurosci [Internet]. 2015 Feb 20 [cited 2017 Aug 22]; 16 (3):147–58. Available from: http://www.nature.com/doifinder/10.1038/nrn3900 PMID: 25697158
3. BROWNELL B, HUGHES JT. The distribution of plaques in the cerebrum in multiple sclerosis. J Neurol Neurosurg Psychiatry [Internet]. 1962 Nov [cited 2017 Aug 22]; 25:315–20. Available from: http://www.ncbi.nlm.nih.gov/pubmed/14016083 PMID: 14016083
4. Chard DT, Griffin CM, Parker GJM, Kapoor R, Thompson AJ, Miller DH. Brain atrophy in clinically early relapsing-remitting multiple sclerosis. Brain [Internet]. 2002 Feb [cited 2017 Aug 22]; 125(Pt 2):327–37. Available from: http://www.ncbi.nlm.nih.gov/pubmed/11844733 PMID: 11844733
5. Dalton CM, Chard DT, Davies GR, Miszkiel KA, Altmann DR, Fernando K, et al. Early development of multiple sclerosis is associated with progressive grey matter atrophy in patients presenting with clinically isolated syndromes. Brain [Internet]. 2004 May 26 [cited 2017 Aug 22]; 127(Pt 5):1101–7. Available from: https://academic.oup.com/brain/article-lookup/doi/10.1093/brain/awh126 PMID: 14998914
6. Chard DT, Griffin CM, Rashid W, Davies GR, Altmann DR, Kapoor R, et al. Progressive grey matter atrophy in clinically early relapsing-remitting multiple sclerosis. Mult Scler [Internet]. 2004 Aug 1 [cited 2017 Aug 22]; 10(4):387–91. Available from: http://www.ncbi.nlm.nih.gov/pubmed/15327034 https://doi.org/10.1191/1352458504ms1050oa PMID: 15327034
7. Gabilondo I, Martínez-Lapiscina EH, Martínez-Heras E, Fraga-Pumar E, Llufriu S, Ortiz S, et al. Trans-synaptic axonal degeneration in the visual pathway in multiple sclerosis. Ann Neurol [Internet]. 2014 Jan [cited 2017 Aug 22]; 75(1):98–107. Available from: http://www.ncbi.nlm.nih.gov/pubmed/24114885 https://doi.org/10.1002/ana.24030 PMID: 24114885

8. Martínez-Lapiscina EH, Sanchez-Dalmau B, Fraga-Pumar E, Ortiz-Perez S, Tercero-Uribe AI, Torres-Torres R, et al. The visual pathway as a model to understand brain damage in multiple sclerosis. Mult Scler J [Internet]. 2014 Nov 10 [cited 2017 Aug 22]; 20(13):1678–85. Available from: http://www.ncbi.nlm.nih.gov/pubmed/25013155
9. Sinnecker T, Oberwahrenbrock T, Metz I, Zimmermann H, Pfueller CF, Harms L, et al. Optic radiation damage in multiple sclerosis is associated with visual dysfunction and retinal thinning—an ultrahigh-field MR pilot study. Eur Radiol [Internet]. 2015 Jan 17 [cited 2017 Aug 22]; 25(1):122–31. Available from: http://link.springer.com/10.1007/s00330-014-3358-8 PMID: 25129119
10. Klistorner A, Sriram P, Vootakuru N, Wang C, Barnett MH, Garrick R, et al. Axonal loss of retinal neurons in multiple sclerosis associated with optic radiation lesions. Neurology [Internet]. 2014 Jun 17 [cited 2017 Aug 22]; 82(24):2165–72. Available from: http://www.neurology.org/cgi/doi/10.1212/WNL.0000000000000522 PMID: 24838786
11. Scheel M, Finke C, Oberwahrenbrock T, Freing A, Pech L-M, Schlichting J, et al. Retinal nerve fibre layer thickness correlates with brain white matter damage in multiple sclerosis: a combined optical coherence tomography and diffusion tensor imaging study. Mult Scler [Internet]. 2014 Dec 19 [cited 2017 Aug 22]; 20(14):1904–7. Available from: http://journals.sagepub.com/doi/10.1177/1352458514535128 PMID: 24842962
12. Balk LJ, Steenwijk MD, Tewarie P, Daams M, Killestein J, Wattjes MP, et al. Bidirectional trans-synaptic axonal degeneration in the visual pathway in multiple sclerosis. J Neurol Neurosurg Psychiatry [Internet]. 2015 Apr [cited 2017 Aug 22]; 86(4):419–24. Available from: http://jnnp.bmj.com/lookup/doi/10.1136/jnnp-2014-308189 PMID: 24973342
13. Dasenbrock HH, Smith SA, Ozturk A, Farrell SK, Calabresi PA, Reich DS. Diffusion tensor imaging of the optic tracts in multiple sclerosis: association with retinal thinning and visual disability. J Neuroimaging [Internet]. 2011 Apr [cited 2017 Aug 22]; 21(2):e41–9. Available from: https://doi.org/10.1111/j.1552-6569.2010.00468.x PMID: 20331501
14. Raz N, Bick A, Ben-Hur T, Levin N. Focal demyelinative damage and neighboring white matter integrity: an optic neuritis study. Mult Scler J [Internet]. 2015 Apr 28 [cited 2017 Aug 22]; 21(5):562–71. Available from: http://journals.sagepub.com/doi/10.1177/1352458514551452
15. Polman CH, Reingold SC, Banwell B, Clanet M, Cohen JA, Filippi M, et al. Diagnostic criteria for multiple sclerosis: 2010 Revisions to the McDonald criteria. Ann Neurol [Internet]. 2011 Feb [cited 2017 Mar 20]; 69(2):292–302. Available from: http://www.ncbi.nlm.nih.gov/pubmed/21387374 PMID: 21387374
16. Hodel J, Outteryck O, Bocher A-L, Zéphir H, Lambert O, Benadjaoud MA, et al. Comparison of 3D double inversion recovery and 2D STIR FLAIR MR sequences for the imaging of optic neuritis: pilot study. Eur Radiol [Internet]. 2014 Dec 23 [cited 2017 Aug 22]; 24(12):3069–75. Available from: http://link.springer.com/10.1007/s00330-014-3342-3 PMID: 25149294
17. Hadhoum N, Hodel J, Defoort-Dhellemmes S, Duhamel A, Drumez E, Zéphir H, et al. Length of optic nerve double inversion recovery hypersignal is associated with retinal axonal loss. Mult Scler [Internet]. 2016 Apr 30 [cited 2017 Aug 22]; 22(5):649–58. Available from: http://journals.sagepub.com/doi/10.1177/1352458515598021 PMID: 26227005
18. Tewarie P, Balk L, Costello F, Green A, Martin R, Schippling S, et al. The OSCAR-IB consensus criteria for retinal OCT quality assessment. Villoslada P, editor. PLoS One [Internet]. 2012 Apr 19 [cited 2017 Aug 22]; 7(4):e34823. Available from: http://dx.plos.org/10.1371/journal.pone.0034823 PMID: 22536333
19. Schippling S, Balk L, Costello F, Albrecht P, Balcer L, Calabresi P, et al. Quality control for retinal OCT in multiple sclerosis: validation of the OSCAR-IB criteria. Mult Scler J [Internet]. 2015 Feb 16 [cited 2017 Aug 22]; 21(2):163–70. Available from: http://www.ncbi.nlm.nih.gov/pubmed/24948688
20. Toosy AT, Mason DF, Miller DH. Optic neuritis. Lancet Neurol [Internet]. 2014 Jan [cited 2017 Aug 22]; 13(1):83–99. Available from: http://www.ncbi.nlm.nih.gov/pubmed/24331795 https://doi.org/10.1016/S1474-4422(13)70259-X PMID: 24331795
21. Magliozzi R, Howell O, Vora A, Serafini B, Nicholas R, Puopolo M, et al. Meningeal B-cell follicles in secondary progressive multiple sclerosis associate with early onset of disease and severe cortical pathology. Brain [Internet]. 2007 Apr 21 [cited 2017 Aug 22]; 130(Pt 4):1089–104. Available from: https://academic.oup.com/brain/article-lookup/doi/10.1093/brain/awm038 PMID: 17438020
22. Lucchinetti CF, Popescu BFG, Bunyan RF, Moll NM, Roemer SF, Lassmann H, et al. Inflammatory Cortical Demyelination in Early Multiple Sclerosis. N Engl J Med [Internet]. 2011 Dec 8 [cited 2017 Aug 22]; 365(23):2188–97. Available from: http://www.ncbi.nlm.nih.gov/pubmed/22150037 https://doi.org/10.1056/NEJMoa1100648 PMID: 22150037
23. Seppi D, Puthenparampil M, Federle L, Ruggero S, Toffanin E, Rinaldi F, et al. Cerebrospinal fluid IL-1β correlates with cortical pathology load in multiple sclerosis at clinical onset. J Neuroimmunol [Internet]. 2014 May 15 [cited 2017 Aug 22]; 270(1–2):56–60. Available from: http://linkinghub.elsevier.com/retrieve/pii/S0165572814000642 https://doi.org/10.1016/j.jneuroim.2014.02.014 PMID: 24657029

24. Rossi S, Furlan R, De Chiara V, Motta C, Studer V, Mori F, et al. Interleukin-1β causes synaptic hyperexcitability in multiple sclerosis. Ann Neurol [Internet]. 2012 Jan [cited 2017 Aug 22]; 71(1):76–83. Available from: http://doi.wiley.com/10.1002/ana.22512 PMID: 22275254

25. Calabrese M, Federle L, Bernardi V, Rinaldi F, Favaretto A, Varagnolo MC, et al. The association of intrathecal immunoglobulin synthesis and cortical lesions predicts disease activity in clinically isolated syndrome and early relapsing-remitting multiple sclerosis. Mult Scler [Internet]. 2012 Feb 25 [cited 2017 Aug 22]; 18(2):174–80. Available from: http://journals.sagepub.com/doi/10.1177/1352458511418550 PMID: 21868488

26. Calabrese M, Atzori M, Bernardi V, Morra A, Romualdi C, Rinaldi L, et al. Cortical atrophy is relevant in multiple sclerosis at clinical onset. J Neurol [Internet]. 2007 Sep 14 [cited 2017 Aug 22]; 254(9):1212–20. Available from: http://www.ncbi.nlm.nih.gov/pubmed/17361339 https://doi.org/10.1007/s00415-006-0503-6 PMID: 17361339

27. Trapp BD, Peterson J, Ransohoff RM, Rudick R, Mörk S, Bö L. Axonal Transection in the Lesions of Multiple Sclerosis. N Engl J Med [Internet]. 1998 Jan 29 [cited 2017 Aug 22]; 338(5):278–85. Available from: http://www.ncbi.nlm.nih.gov/pubmed/9445407 https://doi.org/10.1056/NEJM199801293380502 PMID: 9445407

28. Mitjana R, Tintoré M, Rocca MA, Auger C, Barkhof F, Filippi M, et al. Diagnostic value of brain chronic black holes on T1-weighted MR images in clinically isolated syndromes. Mult Scler [Internet]. 2014 Oct 27 [cited 2017 Aug 22]; 20(11):1471–7. Available from: http://journals.sagepub.com/doi/10.1177/1352458514526083 PMID: 24576831

29. Sepulcre J, Goñi J, Masdeu JC, Bejarano B, Vélez de Mendizábal N, Toledo JB, et al. Contribution of white matter lesions to gray matter atrophy in multiple sclerosis: evidence from voxel-based analysis of T1 lesions in the visual pathway. Arch Neurol [Internet]. 2009 Feb 1 [cited 2017 Aug 22]; 66(2):173–9. Available from: http://archneur.jamanetwork.com/article.aspx?doi=10.1001/archneurol.2008.562 PMID: 19204153

30. Freund P, Weiskopf N, Ward NS, Hutton C, Gall A, Ciccarelli O, et al. Disability, atrophy and cortical reorganization following spinal cord injury. Brain [Internet]. 2011 Jun [cited 2017 Aug 22]; 134(6):1610–22. Available from: http://www.ncbi.nlm.nih.gov/pubmed/21586596

31. Dziedzic T, Metz I, Dallenga T, König FB, Müller S, Stadelmann C, et al. Wallerian degeneration: a major component of early axonal pathology in multiple sclerosis. Brain Pathol [Internet]. 2010 Sep 14 [cited 2017 Aug 22]; 20(5):976–85. Available from: http://doi.wiley.com/10.1111/j.1750-3639.2010.00401.x PMID: 20477831

32. Rocca MA, Mesaros S, Preziosa P, Pagani E, Stosic-Opincal T, Dujmovic-Basuroski I, et al. Wallerian and trans-synaptic degeneration contribute to optic radiation damage in multiple sclerosis: a diffusion tensor MRI study. Mult Scler [Internet]. 2013 Oct 9 [cited 2017 Aug 22]; 19(12):1610–7. Available from: http://journals.sagepub.com/doi/10.1177/1352458513485146 PMID: 23572238

33. Enzinger C, Barkhof F, Ciccarelli O, Filippi M, Kappos L, Rocca MA, et al. Nonconventional MRI and microstructural cerebral changes in multiple sclerosis. Nat Rev Neurol [Internet]. 2015 Dec 3 [cited 2017 Aug 22]; 11(12):676–86. Available from: http://www.nature.com/doifinder/10.1038/nrneurol.2015.194 PMID: 26526531

34. Steenwijk MD, Daams M, Pouwels PJW, Balk LJ, Tewarie PK, Killestein J, et al. What explains gray matter atrophy in long-standing multiple sclerosis? Radiology [Internet]. 2014 Sep [cited 2017 Aug 22]; 272(3):832–42. Available from: http://pubs.rsna.org/doi/10.1148/radiol.14132708 PMID: 24761837

35. Jonkman LE, Soriano AL, Amor S, Barkhof F, van der Valk P, Vrenken H, et al. Can MS lesion stages be distinguished with MRI? A postmortem MRI and histopathology study. J Neurol [Internet]. 2015 Apr 13 [cited 2017 Aug 22]; 262(4):1074–80. Available from: http://link.springer.com/10.1007/s00415-015-7689-4 PMID: 25761376

36. Evangelou N, Konz D, Esiri MM, Smith S, Palace J, Matthews PM. Size-selective neuronal changes in the anterior optic pathways suggest a differential susceptibility to injury in multiple sclerosis. Brain [Internet]. 2001 Sep [cited 2017 Aug 22]; 124(Pt 9):1813–20. Available from: http://www.ncbi.nlm.nih.gov/pubmed/11522583 PMID: 11522583

37. Ciccarelli O, Toosy AT, Hickman SJ, Parker GJM, Wheeler-Kingshott CAM, Miller DH, et al. Optic radiation changes after optic neuritis detected by tractography-based group mapping. Hum Brain Mapp [Internet]. 2005 Jul [cited 2017 Aug 22]; 25(3):308–16. Available from: http://doi.wiley.com/10.1002/hbm.20101 PMID: 15834863